

Enhancing The Electrical Conductivity by Graphene Growing on Nickel Electroplated Bolts by Chemical Vapor Deposition (CVD) Technique

Etkin CAN*, Metehan ATAGÜR

Abstract

The increasing popularity of electric vehicles in recent years brings different demands in the automotive industry. Even the simplest components in EV such as bolts and nuts require new technologies to meet customer demands. Conductive coatings are one of the examples of such demands in order to get rid of the load accumulation that may occur inside the vehicle by grounding.

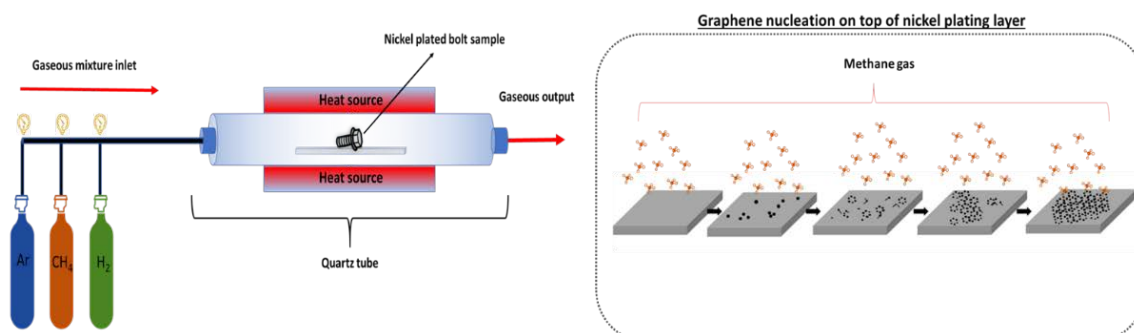
Thanks to the high electrical conductivity of copper, electrolytic copper plating process for fasteners is widely used for such applications. However, electrolytic copper coating brings disadvantages such as low corrosion resistance that brings fast darkening as a result of oxidation and galvanic corrosion that may occur due to the fact that the opposite part is a different metal.

In this study, graphene was grown on electrolytic pure nickel-plated bolts by chemical vapor deposition (CVD) method. RAMAN analyses were performed to confirm graphene formation on nickel-plated samples. Graphene coated samples were tested in Norm coating in electrically conductive SCANIA STD 4472 setup. To evaluate the corrosion resistance, ISO 9227 salt spray test was performed.

Keywords: Chemical vapor deposition (CVD), Graphene, Electric vehicles (EVs), Electroplating

*Corresponding Author Email: etkinan@windowslive.com, etkin.can@normcoating.com

Graphical Abstract



1. Introduction

As the automotive industry undergoes a transformative shift towards electric vehicles (EVs), the demand for advanced technologies within the sector has surged (Sampaio et al., 2022). This paradigm shift necessitates a reevaluation of even the most fundamental components, such as bolts and nuts, prompting the exploration of innovative solutions to address the evolving needs of consumers. A notable challenge in the domain of electric vehicles is the management of electrical load distribution within the vehicle, a concern that extends to the intricacies of grounding (Duan et al., 2019; Hunt et al., 2022; Park et al., 2011).

Conventionally, the use of electrolytic chrome, copper and tin plating has been pivotal in enhancing the electrical conductivity of fasteners, especially those deployed in critical areas like the engine and battery components. However, the widespread adoption of electrolytic copper and tin coatings has not been without its limitations. Notably, the propensity for rapid tarnishing due to oxidation and the susceptibility to galvanic corrosion, particularly when in contact with dissimilar metals, pose significant drawbacks to this traditional approach (Anderson, 1993; Aziz Ameen et al., 2010; S. L. Hingley, 2013; S. Hingley & Oduoza, 2011; Weisenberger & Durkin, 1994).

The electrical conductivity of fasteners and vehicle components holds paramount importance in ensuring effective grounding within automotive systems. This necessity is particularly heightened in electric vehicles, where establishing a robust grounding system is critical for both safety and optimal functionality. To meet this demand, conductive coatings featuring materials like tin or graphene are employed to augment the electrical conductivity of these components (Chemartin et al., 2013; G & C, 1997; Kurth et al., 2015; Yin et al., 2016).

In the automotive sector, the significance of graphene-based coatings is noteworthy. These coatings play a pivotal role in enhancing the structural, thermal, and electrical attributes of the underlying substrate. This multifaceted improvement contributes not only to the efficiency and safety of the vehicle but also replicates a metallic-like appearance. This is a noteworthy departure from traditional conductive platings, signaling a transformative shift in the way electrical conductivity is integrated into automotive design (Barkan, 2023; Das & Chaudhary, 2021; Dericiler et al., 2022; Elmarakbi & Azoti, 2018; Kadirgama et al., 2023).

In response to these challenges, the present study investigates a novel approach by employing graphene in conductive coating applications for fasteners. Graphene, a two-dimensional carbon allotrope, exhibits exceptional electrical conductivity, surpassing that of copper by 70-85%. This distinctive property positions graphene as a promising candidate for the development of innovative fastener coatings capable of meeting the heightened electrical conductivity demands arising in the wake of EV proliferation (Köhne, 2011; Rizzi et al., 2020).

In this pursuit, we focus on the chemical vapor deposition (CVD) method to grow graphene on electrolytic pure nickel-plated bolts, presenting a viable alternative to traditional copper-coated counterparts. Rigorous analysis, including Raman spectroscopy, is employed to ascertain the successful formation of graphene on the nickel-plated samples. Subsequently, the graphene-coated samples undergo testing within a SCANIA STD 4472 electrically conductive setup to assess their performance within a norm coating environment.

This research extends its examination to the corrosion resistance of the graphene-coated fasteners through the implementation of ISO 9227 salt spray tests. Through these comprehensive evaluations, we aim to contribute to the ongoing discourse on advancing conductive coating technologies, providing a nuanced understanding of the potential benefits and challenges associated with integrating graphene into fastener applications within electric vehicles.

2. Materials and Methods

2.1 Materials

Norm Coating company supplied M8 x 75 mm bolt samples with a strength classification of 10.9. The electrolytic plating method was utilized to coat the bolts with pure nickel. The bolts are composed of 23MnB4 steel, and Table 1 provides the elemental composition of the 23MnB4 material.

Table 1. 23MnB4 steel chemical composition content (Database, 2025)

| Element | Content (wt. %) |
|---------|-----------------|
| Fe | 97-98.1 |
| Mn | 0.9 - 1.2 |
| C | 0.2 - 0.25 |
| Si | 0.3 |
| P | 0.025 |
| S | 0.025 |
| Cr | 0.3 |
| Cu | 0.25 |
| B | 0.0008 - 0.005 |

For interim protection, a coating of paraffin oil was applied to the bolt samples. Prior to the application of the Chemical Vapor Deposition (CVD) coating, the provisional protective oil was dissolved using the ultrasonic method in acetone. Subsequently, the cleaned samples were subjected to drying in an oven at 50 °C.

2.2 Methods

2.2.1 Chemical vapor deposition (CVD)

The thermal processing regimen was initiated with the elevation of the oven temperature from ambient conditions to 1000 °C within a duration of 50 minutes. Subsequently, the system was maintained at 1000 °C for a specified interval of 40 minutes to create an optimal thermal environment for the ensuing chemical vapor deposition (CVD) process. During the CVD phase, a controlled introduction of methane (CH₄) gas was orchestrated for a precise period of 10 minutes.

The gas feeding parameters were meticulously configured to achieve optimal conditions for the growth of graphene. Argon (Ar) was introduced at a flow rate of 1000 standard cubic centimeters per minute (sccm), providing a controlled inert atmosphere. Simultaneously, hydrogen (H₂) was incorporated at a rate of 60 sccm, contributing to the reduction of metal catalysts and facilitating the overall growth process. The crucial carbon precursor, methane (CH₄), was introduced at a flow rate of 30 sccm, serving as the primary carbon source for graphene synthesis.

Following the graphene growth phase, a rapid cooling procedure was swiftly implemented for the samples. This meticulously designed thermal profile and gas composition ensure the controlled and reproducible synthesis of graphene on the substrate, a fundamental aspect of the chemical vapor deposition methodology employed in this study.

2.2.2 Characterization

The investigation into graphene formation was executed utilizing the Renishaw Raman Spectrometer, covering a spectral range of 260-3300 cm⁻¹. Raman spectroscopy served as the primary analytical tool, enabling the meticulous examination of the characteristic G and 2D bands associated with graphene. The objective was to unequivocally confirm the successful synthesis of graphene on nickel-plated bolts through the Chemical Vapor Deposition (CVD) method. Concurrently, the Raman analysis facilitated the exploration of diverse parameters influencing the intricate process of graphene synthesis.

Subsequent to the Raman analysis, X-ray Diffraction (XRD) investigations were carried out employing the Panalytical Empyrean XRD instrument equipped with a Cu anode. The scanning rate was meticulously set at 0.01°/s over a range spanning 5° to 90°. This comprehensive XRD analysis aimed to discern the crystalline phase formations within the graphene coatings, providing insights into the structural influence of graphene on nickel-plated bolt samples.

The ISO 9227 Salt Spray Test, executed in accordance with standardized protocols, transpired within the salt spray chamber of the Norm Coating Quality Control Unit. Maintaining a controlled atmosphere and temperature, a solution comprising pure water and 5% NaCl was systematically sprayed onto the test plates at

predefined intervals. Observations were focused on monitoring the progression of white or red rust over 24-hour intervals, offering valuable corrosion resistance insights.

The examination of graphene growth on bolt samples was further elucidated through Scanning Electron Microscopy (SEM) analysis. The Carl Zeiss 300VP SEM, operating at a fixed acceleration voltage of 5.0 kV, facilitated high-resolution imaging of graphene-coated surfaces. Complementing this, Energy-Dispersive X-ray Spectroscopy (EDS) analysis provided elemental composition verification of the graphene coatings on nickel-plated bolt samples.

Concurrently, the electrical conductivity assessment of the bolts adhered meticulously to the STD 4472 standard. The foundational element for this measurement setup was a powder-coated steel plate, equipped with weld nuts strategically positioned at regular intervals. The procedural methodology involved the affixing of screws into adjacent weld nuts, with a cable terminal crimped using a $\varnothing 16$ mm cable securely positioned between the screw and the steel plate. In cases requiring precise clamping length, an isolating plate was introduced between the cable terminal and the steel plate. Utilizing a manual torque wrench, preset at an assembly torque of 34 Nm for all bolt variations, the screws were securely tightened.

Following the tightening phase, a continuous current of 80 A was systematically passed through both the bolts and the steel plate. The subsequent measurement of the resistance of the bolts was achieved by evaluating the voltage drop across two bolts connected by a steel bearing plate. The resistance of the bolt sample was then calculated according to Ohm's law ($R_{\text{fastener}} = (U_{C2} - C1) / I$). This comprehensive test setup deviates from the prior approach by introducing distinct parameters and procedural adjustments, offering a nuanced perspective on the electrical conductivity assessment of the bolts.

3. Results and Discussion

3.1 Raman spectroscopic analysis (RAMAN)

The results of the Raman analysis, providing insights into the graphene structure on nickel-plated bolt samples grown through the CVD method, are visually represented in Figure 1.

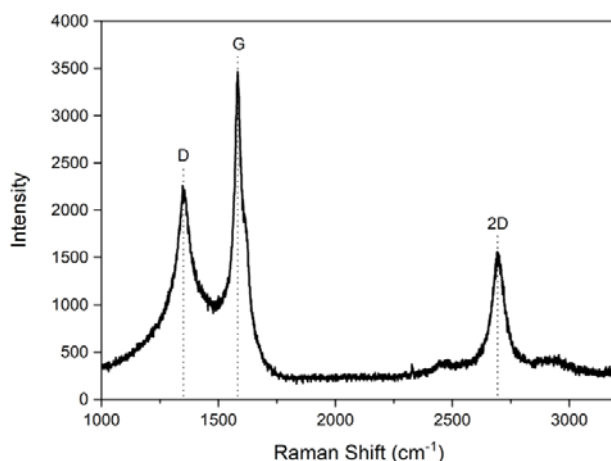


Figure 1. The Raman results of graphene coated on nickel-plated bolt samples

In the Raman spectroscopic analysis conducted on the nickel-plated bolt samples subjected to the Chemical Vapor Deposition (CVD) method for graphene growth, an excitation source of 532 nm was employed. The acquired spectra revealed three prominent Raman features indicative of the graphene structure.

The first and foremost feature is the G band, peaking at approximately 1580 cm^{-1} , corresponding to in-plane vibrations of sp^2 carbon atoms. The second feature is the 2D band, situated at around 2700 cm^{-1} , representing a second-order Raman process associated with graphitic sp^2 materials. The third significant band

is the D band, detected at approximately 1300 cm^{-1} , indicating disordered carbon atoms or graphene edges—a characteristic defect band. Analysis of the obtained spectra suggests the presence of few-layer graphene, as evidenced by the calculated 2D/G ratio of 0.45, which is smaller than 1. This ratio serves as an indicator of the number of graphene layers, with values less than 1 signifying a multilayered structure (Childres et al., n.d.; Ferrari & Basko, 2013). The observed D band, while contributing to the overall spectrum, suggests potential impurities or reduced crystallinity, potentially influenced by the underlying material. The prioritization of the D peak in the spectrum may imply the presence of defects or lower crystallinity, a feature that could be attributed to the underlying substrate. Ideally, the absence or reduced prominence of the D peak would have been preferable, indicating a higher-quality graphene synthesis. Nevertheless, the obtained 2D/G ratio of 0.45 is consistent with the intentional synthesis of multilayer graphene on nickel substrates, aligning with the anticipated and desired outcome of the experiment (Malard et al., 2009; Ni et al., 2008).

3.2 X-ray diffraction (XRD)

The X-ray Diffraction (XRD) outcomes for Nickel-plated, graphene-coated, and untreated bolt samples are presented in Figure 2. Notably, the XRD peaks observed in both the Ni-coated and graphene-coated samples closely resembled the patterns documented in the JCPDS card no. 47-1049, indicative of pure NiO powder. It is pertinent to note that the NiO peak at $2\theta \sim 44^\circ$ coincided with the prominent peak attributed to the Fe substrate (Liu et al., 2017).

Additionally, distinct XRD peaks at 24.89° , 34.02° , 36.55° , 41.88° , and 55.24° were identified, aligning with the characteristic peaks of graphene oxide as reported by Mansoori et al. [5]. Importantly, these discernible peaks were consistent across the XRD spectra of the graphene-coated samples. This correlation further substantiates the successful integration of graphene onto the bolt samples, offering valuable insights into the structural characteristics of the synthesized graphene coatings (Kuang et al., 2013a; Ren et al., 2015; Stobinski et al., 2014; Surekha et al., 2020).

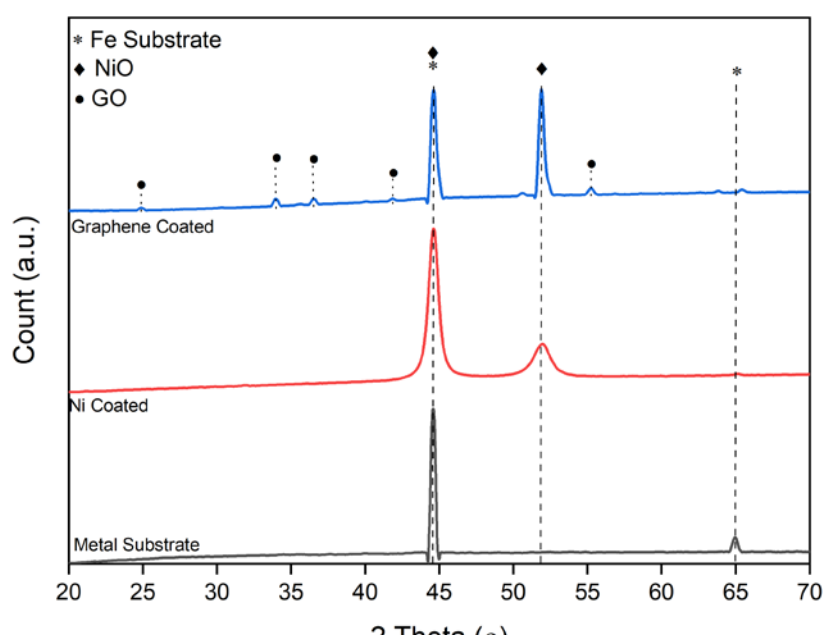


Figure 2. XRD result of Ni-plated, graphene coated and untreated bolt samples

3.3 Energy-Dispersive X-ray Spectroscopy (EDS)

In Figure 3, SEM-EDS results provide insights into the surface characteristics of the nickel-plated bolt samples. Figure 3(b) depicts the nickel electroplated surface, exhibiting a smooth and anomaly-free appearance. Conversely, Figure 3(a) showcases the bolt sample coated with electrolytic nickel through the CVD method. While the surface maintains similarity to Figure 3(b), distinctive dark-colored phases emerge in

random areas, indicating the inability of the CVD method to yield a homogeneous coating. These carbon-like structures are observed to deposit selectively in specific regions. To further confirm the composition of the prepared graphene on Ni-plated coatings, Energy Dispersive Spectroscopy (EDS) analysis was employed. The EDS results, as depicted in Figure 3(c), affirm the presence of Ni and C, substantiating the successful incorporation of graphene into the nickel matrix during the deposition process. Notably, impurities such as Cl, Mn, and Na were detected in the structure, indicating potential contaminants. Moreover, a notable increase in O₂ content suggests the initiation of surface oxidation. The region exhibiting high carbon content corresponds to the area where carbon allotropes, including graphene, were deposited successfully by the CVD method. Upon detailed examination, the SEM image of the black region reveals a transparent structure, indicative of the layered nature of the graphene growth process. The presence of multiple layers in these regions is attributed to the depth of their structure, confirming the successful synthesis of graphene through the CVD method. This comprehensive SEM-EDS analysis elucidates the heterogeneous nature of the graphene coating, shedding light on the distribution of carbon allotropes and potential impurities within the synthesized structure (Kuang et al., 2013b; Peng et al., 2022; Van Hau et al., 2020; Yasin et al., 2018).

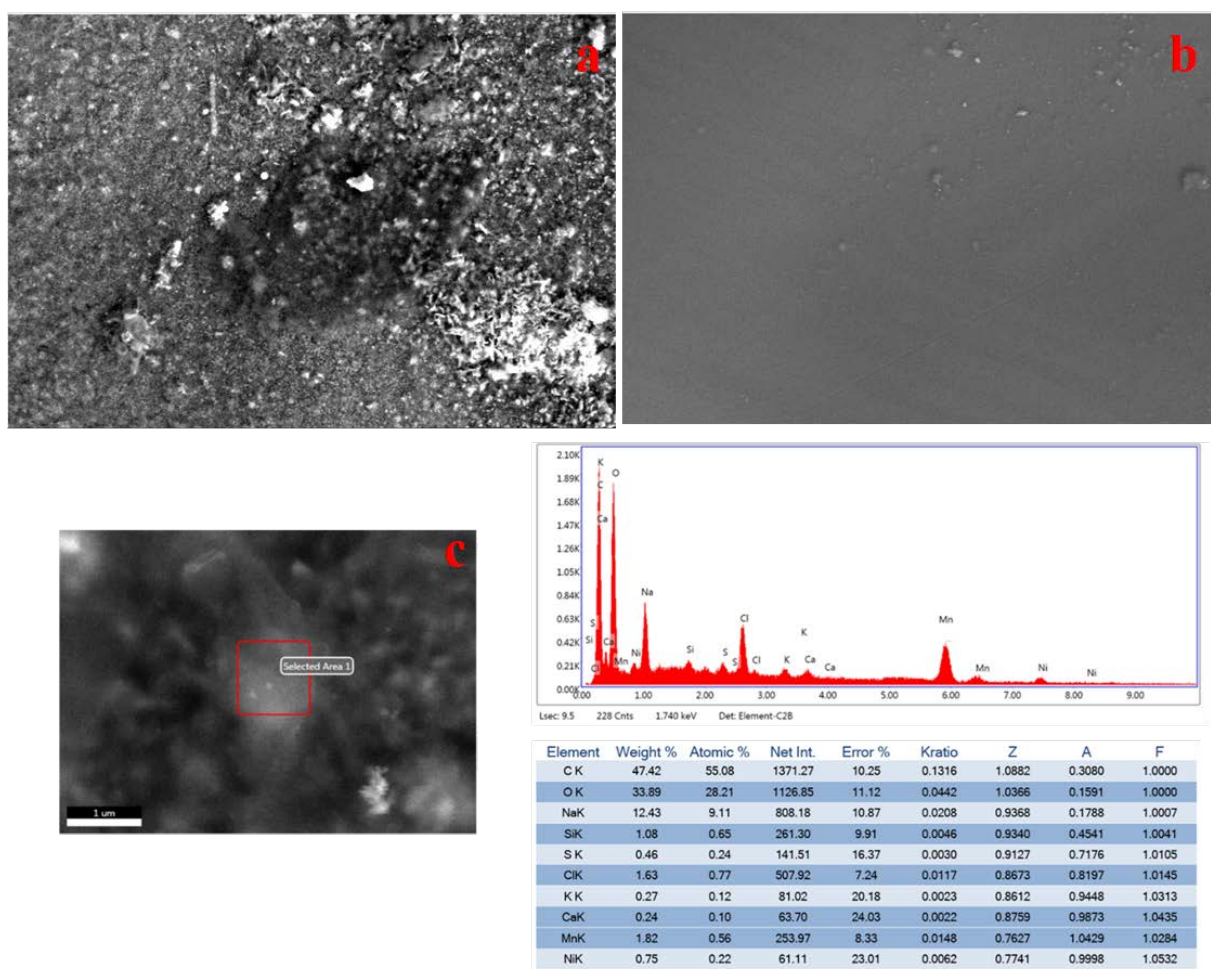


Figure 3. SEM images of CVD graphene coated (a) (x5.000 magnification), Ni-plated (b) (x5.000 magnification), and EDS analysis of CVD graphene coated surface (c)

3.4 ISO 9227 Salt Spray Test

The experimental investigation involved subjecting Ni-plated 23MnB4 steel samples to the ISO 9227 salt spray test, with and without graphene coating, as illustrated in Figure 4. In adherence to established standards, this test exposed the samples to a corrosive 5% NaCl solution, administered at specific angles and intervals. The assessment, conducted at 24-hour intervals, aimed to systematically track signs of corrosion, emphasizing

According to the ISO 9227 salt spray test results, red rust formation was observed on the graphene-coated bolt sample at the 48th hour, whereas the pure electrolytic nickel-coated sample exhibited red rust at the 72nd hour. This outcome implies that the graphene grown on the nickel surface via the CVD method exhibits lower corrosion resistance compared to the non-graphene nickel-plated surface. This phenomenon can be attributed to the non-uniform distribution of graphene observed in the SEM results, suggesting that the entire surface does not homogeneously hold graphene.

[illegible]

| | |
|--|--------|
| White oxidation was observed at <i>Beyaz oksidin görüldüğü süre</i> | |
| Red oxidation was observed at <i>Kırmızı oksidin görüldüğü süre</i> | 48 hrs |
| Test duration <i>Test süresi</i> | |

[illegible]

| | |
|--|--------|
| White oxidation was observed at <i>Beyaz oksidin görülmesi sure</i> | |
| Red oxidation was observed at <i>Kırmızı oksidin görülmesi sure</i> | 72 hrs |
| Test duration | |



3.5 STD 4472 SCANIA electrical conductivity test

Upon scrutinizing the averages of electrical conductivity and insulation values calculated in accordance with Ohm's laws, notable trends emerge. Remarkably, no substantial difference is discerned between the pure steel sample and the electrolytic nickel-coated sample. However, a distinctive contrast arises with the sample wherein graphene was grown using the CVD method, showcasing an electrical conductivity value four times higher than that of the other two samples. This observation underscores the significant impact of the graphene coating on enhancing the electrical conductivity of the nickel-plated bolts, presenting a noteworthy outcome

with potential implications for advanced applications in the automotive industry and related fields (Vallien, 2018).

Table 2. Scania STD 4472 Conductivity Test results of Ni-plated, graphene coated and untreated bolt samples.

| Sample | Scania STD 4472 Conductivity Test | | | | | |
|------------------------|-----------------------------------|--------------------|--------------------------------|------------------------------|--|--|
| | $L_{(A-B)}$ | A | R_s | ρ | σ | $\bar{x} (\sigma)$ |
| | [cm] | [cm ²] | [$\Omega \cdot \text{cm}^2$] | [$\Omega \cdot \text{cm}$] | [$\Omega^{-1} \cdot \text{cm}^{-1}$] | [$\Omega^{-1} \cdot \text{cm}^{-1}$] |
| Steel Fastener | 6,25 | 34,30 | 6,80 | 1,09 | 0,92 | 0,91 |
| | 6,25 | 34,30 | 7,10 | 1,14 | 0,88 | |
| | 6,25 | 34,30 | 6,60 | 1,06 | 0,95 | |
| | 6,25 | 34,30 | 6,90 | 1,10 | 0,91 | |
| Nickel Electroplated | 6,25 | 34,30 | 5,90 | 0,94 | 1,06 | 1,06 |
| | 6,25 | 34,30 | 5,30 | 0,85 | 1,18 | |
| | 6,25 | 34,30 | 6,50 | 1,04 | 0,96 | |
| | 6,25 | 34,30 | 5,90 | 0,94 | 1,06 | |
| CVD-Graphene on plated | 6,25 | 34,30 | 1,53 | 0,24 | 4,08 | 4,00 |
| | 6,25 | 34,30 | 1,64 | 0,26 | 3,81 | |
| | 6,25 | 34,30 | 1,50 | 0,24 | 4,17 | |
| | 6,25 | 34,30 | 1,58 | 0,25 | 3,96 | |

4. Conclusion

In conclusion, the Raman analysis revealed a calculated 2D/G ratio of 0.45, indicating the synthesis of multilayer graphene, given that the ratio was smaller than 1. The corroborating X-ray Diffraction (XRD) and Energy-Dispersive X-ray Spectroscopy (EDS) analyses provided additional support for the presence of graphene on the surface of the Ni-coated substrate.

Significantly, the outcomes of the salt spray test demonstrated a notable reduction of approximately 50% in the corrosion rate for the graphene-coated sample compared to the Ni-coated sample. This underscores the enhanced corrosion resistance imparted by the graphene coating, showcasing its potential for protective applications in challenging environments.

Furthermore, the electrical conductivity test results revealed a substantial increase of approximately 4 times in the electrical conductivity of the graphene-coated sample compared to the reference. This augmentation in electrical conductivity signifies the effectiveness of the graphene coating in improving the overall conductive properties of the coated bolts.

Collectively, these findings underscore the successful synthesis and application of graphene coatings on Ni-coated bolt substrates, showcasing its multifaceted advantages in corrosion resistance and electrical conductivity. The demonstrated improvements position graphene as a promising candidate for advanced coatings in the realm of corrosion protection and conductive applications within the automotive industry and beyond.

Article Information

Conflict of Interest Disclosure: No potential conflict of interest was declared by the authors.

Ethical Approval and Participant Consent: It is declared that scientific and ethical principles were strictly observed during the preparation of this study. All referenced studies and data are properly cited in the bibliography.

Availability of data and materials: Not applicable.

Author's contributions: All authors contributed equally to the design, writing, and revision of this manuscript.

Acknowledgements: The authors would like to thank Prof. Dr. Fethullah Güneş, Çağlar Erdem, Berkay Sallak, Hüseyin Azar and Ogün Sinan Früzbay for their valuable support and contributions to this work.

The authors also express their gratitude to Norm Coating for the technical and moral support provided during the course of this study.

Supporting/Supporting Organizations: This research was supported by the R&D department of Uysal Makine San. İth. İhr. ve Tic. A.Ş., which provided technical assistance and access to laboratory infrastructure. A portion of the analyses was conducted within the company's facilities.

Plagiarism Statement: This article has been scanned by plagiarism detection software, and no instances of plagiarism were found.

5. References

- Anderson, K. J. (1993). Plating Metals. *MRS Bulletin*, 18(1), 57–57. doi: 10.1557/S088376940004349
- Arya, A. K., Raman, R. K. S., Parmar, R., Amati, M., Gregoratti, L., & Saxena, S. (2022). Spectroscopic investigation of improved corrosion resistance of nickel due to multilayer graphene coating developed with suitably tilted substrate during CVD. *Carbon*, 200, 215–226. doi:10.1016/J.CARBON.2022.08.054
- Aziz Ameen, H., Salman Hassan, K., & Rasheed Mohameed, B. (2010). *The effect of electroplating of Cr and Sn on corrosion resistance of low carbon steel (CK15)*. doi:10.5251/ajsir.2010.1.3.565.572
- Barkan, T. (2023). *The Role of Graphene in Achieving e-Mobility in Automotive Applications*. doi:10.4271/EPR2023006
- Chang, W., Wang, P., Zhao, Y., Ren, C., Popov, B. N., & Li, C. (2020). Characterizing corrosion properties of graphene barrier layers deposited on polycrystalline metals. *Surface and Coatings Technology*, 398, 126077. doi: 10.1016/J.SURFCOAT.2020.126077
- Chemartin, L., Lalande, P., & Tristant, F. (2013). *Modeling and simulation of sparking in fastening assemblies*. <https://onera.hal.science/hal-01058554>
- Childres, I., Jauregui, L. A., Park, W., Cao, H., & Chen, Y. P. (n.d.). *Raman Spectroscopy of Graphene and Related Materials*. In: Jang, J.I., Ed., *New Developments in Photon and Materials Research*, NOVA Science Publishers, Inc., New York, 403-418.
- Das, P. P., & Chaudhary, V. (2021). *Application of Graphene-Based Biopolymer Nanocomposites for Automotive and Electronic Based Components*. 311–323. doi: 10.1007/978-981-15-9180-8_17
- Database, N. (2025). 23MnB4 / 1.5535 - steelnumber - chemical composition, equivalent, properties. *Steelnumber.com*. https://www.steelnumber.com/en/steel_composition_eu.php?name_id=734

- Dericiler, K., Aliyeva, N., Mohammadjafari Sadeghi, H., Sas, H. S., Menciloglu, Y. Z., & Saner Okan, B. (2022). Graphene in automotive parts. *Nanotechnology in the Automotive Industry*, 623–651. doi:10.1016/B978-0-323-90524-4.00030-X
- Duan, J., Tang, X., Dai, H., Yang, Y., Wu, W., Wei, X., & Huang, Y. (2019). Building Safe Lithium-Ion Batteries for Electric Vehicles: A Review. *Electrochemical Energy Reviews* 2019 3:1, 3(1), 1–42. doi:10.1007/S41918-019-00060-4
- Elmarakbi, A., & Azoti, W. (2018). State of the Art on Graphene Lightweighting Nanocomposites for Automotive Applications. *Experimental Characterization, Predictive Mechanical and Thermal Modeling of Nanostructures and Their Polymer Composites*, 1–23. doi:10.1016/B978-0-323-48061-1.00001-4
- Ferrari, A. C., & Basko, D. M. (2013). Raman spectroscopy as a versatile tool for studying the properties of graphene. *Nature Nanotechnology* 2013 8:4, 8(4), 235–246. doi: 10.1038/nnano.2013.46
- G, M. D., & C, H. M. (1997, April). *Effect of conductivity between fasteners and aluminum skin on eddy current specimens*. *Osti.gov*. <https://www.osti.gov/biblio/460783>
- Hingley, S. L. (2013). *Characterisation of Potential Replacements for Nickel Compounds used in Decorative Chromium Plating*. <https://wlv.openrepository.com/handle/2436/311675>
- Hingley, S., & Oduoza, C. (2011). An Investigation into a Copper/Tin Alloy as an Underlying Coating to Chromium. *Formerly Part of Journal of Materials Science and Engineering*, 1, 410–420.
- Hunt, G. J., Javaid, R., Simon, J., Peplow, M., & Prengaman, C. (2022). Understanding Conductive Layer Deposits: Test Method Development for Lubricant Performance Testing for Hybrid and Electric Vehicle Applications. *SAE International Journal of Electrified Vehicles*, 12(2), 263–277. doi: 10.4271/14-12-02-0014
- Kadirgama, G., Bin Razman, M. I., Ramasamy, D., Kadirgama, K., & Farhana, K. (2023). Graphene as an Alternative Additive in Automotive Cooling System. *Lecture Notes in Mechanical Engineering*, 13–35. doi:10.1007/978-981-19-1457-7_2
- Köhne, M. (2021, February 3). *Can graphene compete with copper in electrical conductivity?* *Bosch Global*. <https://www.bosch.com/stories/can-graphene-compete-with-copper-in-electrical-conductivity/>
- Kuang, D., Xu, L., Liu, L., Hu, W., & Wu, Y. (2013a). Graphene–nickel composites. *Applied Surface Science*, 273, 484–490. doi:10.1016/J.APSUSC.2013.02.066
- Kuang, D., Xu, L., Liu, L., Hu, W., & Wu, Y. (2013b). Graphene–nickel composites. *Applied Surface Science*, 273, 484–490. doi:10.1016/J.APSUSC.2013.02.066
- Kurth, J. C., Krauss, P. D., McGormley, J. C., & Harper, J. (2015, March 15–19). Accelerated corrosion study of direct-fixation fasteners [Paper presentation]. CORROSION 2015 Conference, Dallas, TX, United States. AMPP. doi:10.5006/C2015-06133
- Liu, Q., Lu, C., & Li, Y. (2017). Controllable synthesis of ultrathin nickel oxide sheets on carbon cloth for high-performance supercapacitors. *RSC Advances*, 7(37), 23143–23148. doi: 10.1039/C6RA27550H
- Malard, L. M., Pimenta, M. A., Dresselhaus, G., & Dresselhaus, M. S. (2009). Raman spectroscopy in graphene. *Physics Reports*, 473(5–6), 51–87. doi:10.1016/J.PHYSREP.2009.02.003
- Ni, Z., Wang, Y., Yu, T., & Shen, Z. (2008). Raman spectroscopy and imaging of graphene. *Nano Research*, 1(4), 273–291. doi:10.1007/S12274-008-8036-1
- Park, O. K., Cho, Y., Lee, S., Yoo, H. C., Song, H. K., & Cho, J. (2011). Who will drive electric vehicles, olivine or spinel? *Energy & Environmental Science*, 4(5), 1621–1633. doi: 10.1039/C0EE00559B

- Peng, Q., Xiong, W., Tan, X., Venkataraman, M., Mahendran, A. R., Lammer, H., Kejzlar, P., & Militky, J. (2022). Effects of ultrasonic-assisted nickel pretreatment method on electroless copper plating over graphene. *Scientific Reports*, 12(1). doi:10.1038/S41598-022-25457-Y
- Ren, Z., Meng, N., Shehzad, K., Xu, Y., Qu, S., Yu, B., & Luo, J. K. (2015). Mechanical properties of nickel-graphene composites synthesized by electrochemical deposition. *Nanotechnology*, 26(6), 065706. Doi: 10.1088/0957-4484/26/6/065706
- Rizzi, L., Wijaya, A. F., Palanisamy, L. V., Schuster, J., Köhne, M., & Schulz, S. E. (2020). Quantifying the influence of graphene film nanostructure on the macroscopic electrical conductivity. *Nano Express*, 1(2), 020035. Doi:10.1088/2632-959X/ABB37A
- Sampaio, R. F. V., Pragana, J. P. M., Clara, R. G., Bragança, I. M. F., Silva, C. M. A., & Martins, P. A. F. (2022). New Self-Clinching Fasteners for Electric Conductive Connections. *Journal of Manufacturing and Materials Processing* 2022, Vol. 6, Page 159, 6(6), 159. doi:10.3390/JMMP6060159
- Stobinski, L., Lesiak, B., Malolepszy, A., Mazurkiewicz, M., Mierzwa, B., Zemek, J., Jiricek, P., & Bieloshapka, I. (2014). Graphene oxide and reduced graphene oxide studied by the XRD, TEM and electron spectroscopy methods. *Journal of Electron Spectroscopy and Related Phenomena*, 195, 145–154. doi: 10.1016/J.ELSPEX.2014.07.003
- Surekha, G., Krishnaiah, K. V., Ravi, N., & Padma Suvana, R. (2020). FTIR, Raman and XRD analysis of graphene oxide films prepared by modified Hummers method. *Journal of Physics: Conference Series*, 1495(1), 012012. doi:10.1088/1742-6596/1495/1/012012
- Szeptycka, B., Gajewska-Midzialek, A., & Babul, T. (2016). Electrodeposition and Corrosion Resistance of Ni-Graphene Composite Coatings. *Journal of Materials Engineering and Performance*, 25(8), 3134–3138. doi:10.1007/S11665-016-2009-4
- Vallien, A. (2018a). *Material characterization of multi layered zn-alloy coatings on fasteners*. <https://kth.diva-portal.org/smash/get/diva2:1283276/FULLTEXT03.pdf>
- Van Hau, T., Van Trinh, P., Hoai Nam, N. P., Van Tu, N., Lam, V. D., Phuong, D. D., Minh, P. N., & Thang, B. H. (2020). Electrodeposited nickel–graphene nanocomposite coating: effect of graphene nanoplatelet size on its microstructure and hardness. *RSC Advances*, 10(37), 22080–22090. doi:10.1039/D0RA03776A
- Van Hau, T., Van Trinh, P., Van Tu, N., Duoc, P. N. D., Phuong, M. T., Toan, N. X., Phuong, D. D., Nam, N. P. H., Lam, V. D., Minh, P. N., & Thang, B. H. (2021). Electrodeposited nickel–graphene nanocomposite coating: influence of graphene nanoplatelet size on wear and corrosion resistance. *Applied Nanoscience (Switzerland)*, 11(5), 1481–1490. doi:10.1007/S13204-021-01780-0
- Weisenberger, L. M., & Durkin, B. J. (1994). Copper Plating. *Surface Engineering*, 167–176. doi: 10.31399/ASM.HB.V05.A0001242
- Yasin, G., Arif, M., Nizam, M. N., Shakeel, M., Khan, M. A., Khan, W. Q., Hassan, T. M., Abbas, Z., Farahbakhsh, I., & Zuo, Y. (2018). Effect of surfactant concentration in electrolyte on the fabrication and properties of nickel-graphene nanocomposite coating synthesized by electrochemical co-deposition. *RSC Advances*, 8(36), 20039–20047. doi:10.1039/C7RA13651J
- Yin, J. J., Li, S. L., Yao, X. L., Chang, F., Li, L. K., & Zhang, X. H. (2016). Lightning Strike Ablation Damage Characteristic Analysis for Carbon Fiber/Epoxy Composite Laminate with Fastener. *Applied Composite Materials*, 23(4), 821–837. doi:10.1007/S10443-016-9487-2
- Yivlialin, R., Bussetti, G., Duò, L., Yu, F., Galbiati, M., & Camilli, L. (2018). CVD Graphene/Ni Interface Evolution in Sulfuric Electrolyte. *Langmuir*, 34(11), 3413–3419. doi: 10.1021/ACS.LANGMUIR.8B00459

Affiliations

ETKİN CAN

ADDRESS: Norm Coating/Uysal Makina San. İth. İhr. ve Tic. A.Ş., İzmir, Türkiye

E-MAIL: etkincan@windowlive.com

ORCID: 0000-0001-8227-2111

METEHAN ATAGÜR

ADDRESS: İzmir Katip Çelebi University, Metallurgical and Materials Engineering Department, İzmir,
Türkiye

E-MAIL: metehan.atagur@ikcu.edu.tr

ORCID: 0000-0002-1916-457X